JACS
JOURNAL OF THE AMERICAN CHEMICAL SOCIETY
Communication
pubs.acs.org/JACS

Can Boron and Nitrogen Co-doping Improve Oxygen Reduction Reaction Activity of Carbon Nanotubes?

Yu Zhao,[†] Lijun Yang,*[,†] Sheng Chen,[†] Xizhang Wang,[†] Yanwen Ma,[‡] Qiang Wu,[†] Yufei Jiang,[†] Weijin Qian,[†] and Zheng Hu*[,†]

[†] Key Laboratory of Mesoscopic Chemistry of MOE and Jiangsu Provincial Lab for Nanotechnology, Institute of Theoretical and Computational Chemistry, School of Chemistry and Chemical Engineering, Nanjing University, 210093 Nanjing, P.R. China

[‡] Jiangsu Key Lab for Organic Electronics and Information Displays, Institute of Advanced Materials, Nanjing University of Posts and Telecommunications, 210046 Nanjing, P.R. China

Supporting Information

ABSTRACT: Two kinds of boron and nitrogen co-doped carbon nanotubes (CNTs) dominated by bonded or separated B and N are intentionally prepared, which present distinct oxygen reduction reaction (ORR) performances. The experimental and theoretical results indicate that the bonded case cannot, while the separated one can, turn the inert CNTs into ORR electrocatalysts. This progress demonstrates the crucial role of the doping microstructure on ORR performance, which is of significance in exploring the advanced C-based metal-free electrocatalysts.

Oxygen reduction reaction (ORR) is a critical process in fuel cells,[1,2] which is normally catalyzed on cathodes by Pt-based catalysts. Its sluggish reaction kinetics requires high Pt loading to ensure the efficiency of the whole system. The limited natural reserves and high price of Pt, together with the issues of instability and deactivation by CO poisoning and crossover effect, have hindered the large-scale application of fuel cells.[3,4] Therefore, great efforts have been devoted to reducing Pt consumption by alloying or structural regulation,[5−9] and searching for non-precious metal[10,11] or even metal-free catalysts for ORR.[12−14]

The sp^2 carbon materials have abundant free-flowing π electrons, which make them potential catalysts for reactions needing electrons, such as ORR. However, these π electrons are too inert to be used directly in ORR. In recent years, it has been revealed that, for N-doped electron-rich carbon nanostructures, the carbon π electrons can be activated by conjugating with the lone-pair electrons from N dopants; thus, O_2 molecules get reduced on the positively charged C atoms neighboring N.[15−20] Very recently, we found that, for B-doped electron-deficient carbon nanotubes (CNTs), the π electrons can also be activated for use in ORR.[21] Specifically, the vacant $2p_z$ orbital of B conjugates with the carbon π system to extract the electrons. These electrons become quite active due to the low electronegativity of B, and thus O_2 molecules are reduced on the positively charged B sites. According to these experimental results and theoretical calculations, we summarized two key factors to transform sp^2 carbon into metal-free ORR electrocatalysts by doping: (1) breaking the electroneutrality of sp^2 carbon to create charged sites favorable for O_2 adsorption despite whether the dopants are electron-rich (as N) or electron-deficient (as B); and (2) activating carbon π electrons for effective utilization by O_2.[21] With this strategy, intuition suggests that co-doping with B and N is a possible route to further optimize the carbon-based metal-free ORR electrocatalysts. Recently there have been a few explorations of B and N co-doped sp^2 carbon materials which demonstrate an irregular variation of ORR activities with respect to the B/N ratios and contents.[22,23] For example, the ORR performance of a certain B and N co-doped graphene is even better than that of a commercial Pt/C catalyst, while some others are much worse despite having higher B and N contents.[23] The peculiar behaviors of B and N dopants in the co-doped sp^2 carbon materials indicate there is some underlying factor yet to be discovered, which is critically related to the performance optimization and doping efficiency.

Indeed, a fundamental issue arises when B and N coexist in sp^2 carbon, i.e., B and N are bonded together or located separately. Due to the compensation effect between the p- and n-type dopants,[24] these two cases correspond to totally different electronic structures, and therefore different conjugation effects within the carbon π system, which eventually leads to distinct ORR activities. Based on this consideration, we have synthesized two kinds of B and N co-doped CNTs by different procedures, which are dominated by either bonded or separated B and N. Electrochemical measurements show that the ORR performance for the bonded case gradually drops to the inert level of the pristine CNTs with increasing the B/N ratio, while the onset potential and current density for the separated case gets better and better with increasing B and N contents. Theoretical calculations reveal that neutralization occurs between the extra electron from N and the vacant orbital from B for the bonded case, leading to unfavorable chemisorption of O_2 on the co-doped CNTs. The experimental and theoretical results jointly indicate that the bonded case can hardly break the inertness of CNTs, while the separated case can turn CNTs into excellent ORR electrocatalysts. These results demonstrate the crucial role of the doping microstructure on ORR performance, which is of significance in

Received: October 26, 2012
Published: January 14, 2013

   dx.doi.org/10.1021/ja310566z | J. Am. Chem. Soc. 2013, 135, 1201−1204

designing and optimizing advanced metal-free electrocatalysts by multi-doping sp^2 carbon nanostructures.

Two different routes were employed to prepare the B and N co-doped CNTs with tunable dopant contents. The first one was to dope B and N sequentially: the B-doped CNTs were first synthesized by chemical vapor deposition (CVD) using the mixture solution of triphenylborane (TPB, as B source), benzene, and ferrocene as precursor and catalyst, and then treated at 400 °C in NH_3 to dope N. By NH_3 post-treatment, the N dopant usually occupies the defective sites;[25] hence the pre-formed B-doping configuration could be preserved, which favors forming the separated B and N. The products from this route are denoted as B_1CNTs-NH_3, B_2CNTs-NH_3, and B_3CNTs-NH_3, with increasing B (0.84−1.93 at%) and N (0.58−2.19 at%) contents. The second route was to dope B and N simultaneously: the B and N co-doped CNTs were directly synthesized by CVD using the mixture solution of TPB (as B source), benzylamine (BA, as N source), and ferrocene as precursor and catalyst. As a Lewis acid, TPB could be complexed by BA (a Lewis base) with a stable B−N bonding configuration, which favors forming the bonded B and N.[26] The products with different dopant contents are denoted as B_1CNTs-BA, B_2CNTs-BA, and B_3CNTs-BA. The N contents in these samples are at the same level within 1.39−1.57 at%, while the B contents gradually increase from 0.35 to 1.68 at%. Apparent morphological differences are observed between B_xCNTs-BA and B_xCNTs-NH_3 (x = 1, 2, 3), suggesting their different microstructures. For comparison, two different N-doped CNTs from these two routes were also prepared and denoted as NCNTs-BA and CNTs-NH_3. (Supporting Information S1−S4)

X-ray photoelectron spectroscopy (XPS) was performed to characterize the contents and configurations of the dopants in the samples, and the typical spectra for B_3CNTs-NH_3 and B_3CNTs-BA are shown in Figure 1. The spectra of both B 1s and N 1s display distinct characteristic peaks for the two samples from the different preparation routes, indicating the totally different chemical states of the B and N dopants.

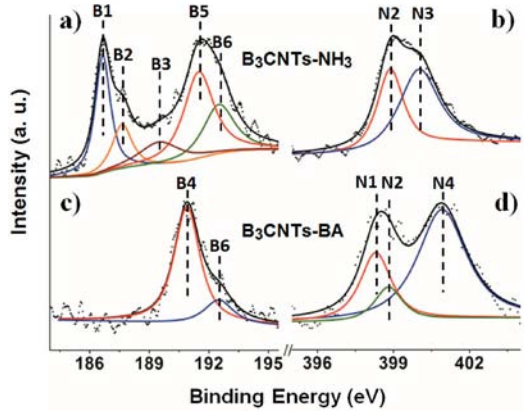

Figure 1. Typical XPS spectra of B 1s (a,c) and N 1s (b,d) of the B and N co-doped samples. Top, B_3CNTs-NH_3; bottom, B_3CNT-BA. B1−B6 correspond to B cluster, B_4C, BC_3, N−B−C moiety, BC_2O, and BCO_2. N1−N4 correspond to N−B−C moiety, pyridinic N, pyrrolic N, and quaternary N.

The B 1s spectrum of B_3CNTs-NH_3 is highly similar to that of the sample before NH_3 treatment, i.e., the B mono-doped CNTs (B_3CNTs) in our previous work,[21] which presents two regions of 186−190 and 190−194 eV, corresponding to the characteristic B−C and O−B−C species (Figure 1a).[21,27] This similarity suggests that the NH_3 post-treatment does not significantly change the B doping configuration, and the later doped N atoms mainly bond with C (Figure S4, Supporting Information). This is also exhibited in the N 1s spectrum of B_3CNTs-NH_3, which is comprised of the typical pyridinic and pyrrolic N's peaked at 398.8 and 400.3 eV, respectively,[25,28,29] without the signal at the lower binding energy around 398.2 eV for N−B bonding (Figure 1b).[30−32] For the samples made by the second route, a series of XPS spectra for B 1s and N 1s is obtained for NCNTs-BA, B_1CNTs-BA, B_2CNTs-BA, and B_3CNTs-BA to check the correlation between N and B dopants. A gradual increase of peak intensity at 398.4 eV is observed with increasing B content, while the N contents stay at the same level (Figure S5, Supporting Information). This clearly indicates that the N 1s peak at 398.4 eV and the major B 1s peak at 191.0 eV can be attributed to the N−B−C moiety (Figure 1c,d).[30−32] The shoulder peak of B 1s at 192.5 eV comes from BCO_2 species (Figure 1c), while the N 1s signals at 398.8 and 401.0 eV come from the pyridinic and quaternary N's, respectively (Figure 1d).

According to the preceding experimental results, two kinds of co-doped CNTs dominated by bonded or separated B and N respectively have been obtained as expected, which demonstrate distinct ORR performances as presented below.

For the B_xCNTs-BA (x = 1, 2, 3) samples featuring bonded B and N, with similar N doping levels (1.39−1.57 at%) but variable B contents (0.35−1.68 at%) (Table S1, Supporting Information), the cyclic voltammetry (CV) and rotating disk electrode (RDE) voltammetry curves are shown in Figure 2,

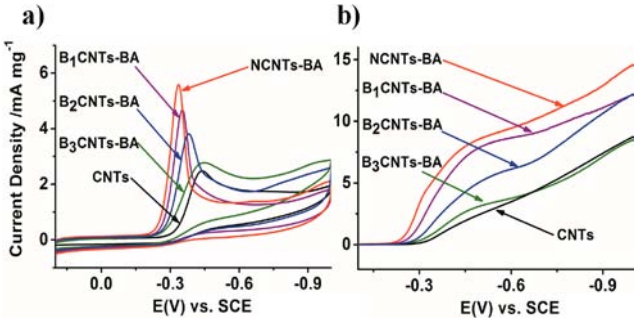

Figure 2. Electrocatalytic capabilities of the BCNTs-BA catalysts for ORR in O_2-saturated 1 mol L^{-1} NaOH electrolyte. (a) CV at a scan rate of 50 mV s^{-1}. (b) RDE at a scan rate of 10 mV s^{-1} and rotation speed of 2500 rpm. CV and RDE curves for pristine CNTs and NCNTs-BA are also presented for comparison. On the vertical scale, 1 mA mg^{-1} corresponds to 0.1 mA cm^{-2}.

referenced to the saturated calomel electrode (SCE) (−0.24 V vs NHE). Corresponding NCNTs-BA (only N dopant) and pristine CNTs were also examined for comparison. Interestingly, the onset and peak potentials as well as the peak currents progressively decrease with increasing the B content in the order of NCNTs-BA, B_1CNTs-BA, B_2CNTs-BA, and B_3CNTs-BA, approaching the level of the pristine CNTs. In this series of samples, increasing B/N ratio means decreasing of the separate N dopant. Therefore, the deterioration of the ORR performances with increasing B/N ratio indicates that the bonded B and N (N−B−C moiety) contribute little to the ORR activity.

For the B_xCNTs-NH_3 (x = 1, 2, 3) samples featuring separated B and N, a monotonic relationship between ORR

dx.doi.org/10.1021/ja310566z | J. Am. Chem. Soc. 2013, 135, 1201−1204

activities and B and N contents is observed from CV and RDE measurements, as shown in Figure 3 (Supporting Information S5). With increasing B and N contents, the maximum peak currents increase obviously from 3.2 ($CNTs\text{-}NH_3$) to 4.1 ($B_1CNTs\text{-}NH_3$), 5.0 ($B_2CNTs\text{-}NH_3$), and 8.9 mA/mg ($B_3CNTs\text{-}NH_3$), accompanied by a progressive positive shift of the peak potentials from −0.38 ($CNTs\text{-}NH_3$) to −0.35 ($B_1CNTs\text{-}NH_3$), −0.34 ($B_2CNTs\text{-}NH_3$), and −0.31 V ($B_3CNTs\text{-}NH_3$) (Figure 3a). Similar evolution is also observed for the steady-state diffusion currents and the onset potentials in RDE voltammetry curves (Figure 3b). The $B_3CNTs\text{-}NH_3$ catalyst with the highest B (1.93 at%) and N (2.19 at%) contents presents the best ORR performance with excellent stability and immunity toward methanol crossover and CO poisoning (Supporting Information S6). Rotating ring-disk electrode (RRDE) measurements show that the transferred electron number (n) per O_2 involved in ORR is 2.5 for $B_3CNTs\text{-}NH_3$, indicating a dominant two-electron process (Supporting Information S7). Therefore, in contrast to the case for the bonded B and N species with little ORR activity, the separated B and N dopants boost the ORR catalytic ability. This clearly demonstrates the significant influence of the doping microstructure on ORR performance.

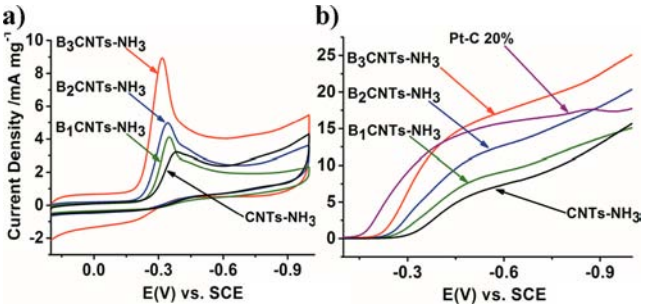

Figure 3. Electrocatalytic capabilities of the $BCNTs\text{-}NH_3$ catalysts for ORR in O_2-saturated 1 mol L^{-1} NaOH electrolyte. (a) CV at a scan rate of 50 mV s^{-1}. (b) RDE at a scan rate of 10 mV s^{-1} and rotation speed of 2500 rpm. CV and RDE curves for $CNTs\text{-}NH_3$ and commercial Pt/C catalyst (20 wt% Pt loading) are also presented for comparison.

The excellent ORR performance for the separated B and N co-doped CNTs is understandable since the mono-B or N doped CNTs have superb ORR activities as revealed by abundant experimental and theoretical studies.[15,18,21,33] In other words, the separation of B and N in the co-doped CNTs can preserve their intrinsic ORR activity. Thus, for the counterpart of the bonded case, the absent ORR activity is academically interesting and practically instructive since it should be avoided in optimizing this kind of advanced electrocatalysts. Therefore, theoretical efforts have been focused on the O_2 adsorption on the bonded B and N co-doped CNTs. Density functional theory (DFT)[34,35] calculations demonstrate that the lowest-energy O_2 adsorption configuration on the co-doped CNT(5,5) has an adsorption distance of 3.30 Å, and the adsorbed O_2 keeps the same bond length (1.21 Å) as the gaseous O_2, indicating a physisorption mode as shown in Figure 4. The highest occupied molecular orbital (HOMO) plot shows a weak interaction between O_2 and the co-doped CNT with little charge transferred to O_2; thus, the O_2 cannot be reduced (Figure 4b).

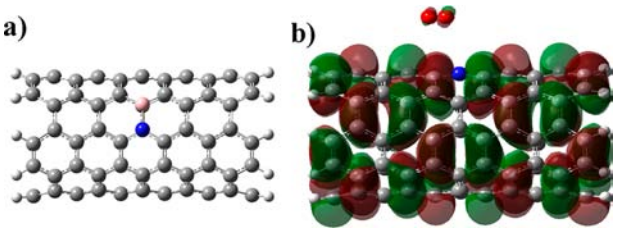

Figure 4. (a) Bonded B and N co-doped CNT(5,5). (b) HOMO plot of the corresponding O_2 adsorption configuration (isodensity value of 0.007 au). N, blue; B, pink; C, black; H, gray; O, red.

The inertness of the bonded B and N co-doped CNT is also revealed by the second-order orbital perturbation analysis for the model in Figure 4a.[36] The results indicate that the lone-pair electrons from N dopant are largely neutralized by the vacant orbital of B dopant, and few electrons or vacant orbitals are left to conjugate with the carbon π system (Supporting Information S8). With little conjugation, the activation of carbon π electrons could hardly occur; thus, the ORR activity becomes like that for the undoped CNT with poor ORR performance. This result is in accordance with the recent report about the B and N co-doping effect on electronic transport by Khalfoun et al., which shows that the bonded B and N are transparent to conduction electrons, and hence the bonded B and N co-doped CNTs act like the pristine ones.[37]

By contrast, the situation for the separated B and N co-doped CNT is totally different. The separation of B from N prevents the neutralization between the electron donor (N) and acceptor (B), so they remain capabile of conjugating with the carbon π system, as in the mono-doped CNTs.[15,21] This is supported by Khalfoun's calculations that the localized transport phenomena for isolated B or N doping are recovered when B and N atoms are far apart in the co-doped CNTs.[37] Hence, the separated B and N co-doped CNTs could demonstrate excellent ORR performance. These results also support the strategy to turn sp^2 carbon into metal-free ORR electrocatalysts by doping, in which the activation of carbon π electrons is a critical step, as proposed in our recent study.[21]

Now we could rationally understand the difference in catalytic ability for the bonded and separated B and N co-doped CNTs demonstrated in the experimental measurements. The neutralization degree between B and N dopants dominates the ORR performances of the B and N co-doped CNTs, which depends on the bonded or separated configuration of the B and N dopants in the C matrix. With this viewpoint, the irregular or peculiar performances of the B and N co-doped carbon nanomaterials could also be speculated.[22,23]

In summary, two kinds of B and N co-doped CNTs dominated by the bonded or separated B and N have been intentionally prepared by CVD growth or post-treatment, respectively, which demonstrate distinct ORR performances. The experimental and theoretical results indicate that the bonded case can hardly break the inertness of CNTs, while the separated one can turn CNTs into excellent ORR electrocatalysts. This progress demonstrates the crucial role of the doping microstructure on ORR performance, which is of significance in designing and optimizing advanced C-based metal-free electrocatalysts for fuel cells. The results in this study also show that the strategy to turn sp^2 carbon into metal-free ORR electrocatalysts deduced from the mono-doped cases[21] is applicable for the multi-doped situations. More attention should be devoted to regulating the dopants' configuration in

dx.doi.org/10.1021/ja310566z | J. Am. Chem. Soc. 2013, 135, 1201−1204

exploring the promising metal-free ORR electrocatalysts of multi-doped carbon nanostructures.

■ ASSOCIATED CONTENT

Supporting Information

Full experimental details; TEM images; BET and XPS data of the products; control experiments, stability tests, and electron transfer number determination for B_3CNTs-NH_3; NBO analysis for the bonded B and N co-doped CNT(5,5). This material is available free of charge via the Internet at http://pubs.acs.org.

■ AUTHOR INFORMATION

Corresponding Author

zhenghu@nju.edu.cn; lijunyang@nju.edu.cn

Notes

The authors declare no competing financial interest.

■ ACKNOWLEDGMENTS

This work was jointly supported by NSFC (20833002, 51232003, 21173114, 21203092, 21173115) and '973' program (2013CB932902).

■ REFERENCES

(1) Gasteiger, H. A.; Marković, N. M. *Science* **2009**, *324*, 48.
(2) Stamenkovic, V. R.; Fowler, B.; Mun, B. S.; Wang, G.; Ross, P. N.; Lucas, C. A.; Marković, N. M. *Science* **2007**, *315*, 493.
(3) Debe, M. K. *Nature* **2012**, *486*, 43.
(4) www.platinum.matthey.com/pgm-prices/price-charts (accessed Oct 26, 2012).
(5) Stamenkovic, V. R.; Mun, B. S.; Arenz, M.; Mayrhofer, K. J. J.; Lucas, C. A.; Wang, G.; Ross, P. N.; Marković, N. M. *Nat. Mater.* **2007**, *6*, 241.
(6) Wang, C.; Daimon, H.; Onodera, T.; Koda, T.; Sun, S. *Angew. Chem., Int. Ed.* **2008**, *47*, 3588.
(7) Alia, S. M.; Zhang, G.; Kisailus, D.; Li, D.; Gu, S.; Jensen, K.; Yan, Y. *Adv. Funct. Mater.* **2010**, *20*, 3742.
(8) Wanjala, B. N.; Fang, B.; Luo, J.; Chen, Y.; Yin, J.; Engelhard, M. H.; Loukrakpam, R.; Zhong, C. J. *J. Am. Chem. Soc.* **2011**, *133*, 12714.
(9) Tian, N.; Zhou, Z. Y.; Sun, S. G.; Ding, Y.; Wang, Z. L. *Science* **2007**, *316*, 732.
(10) Wu, G.; More, K. L.; Johnston, C. M.; Zelenay, P. *Science* **2011**, *332*, 443.
(11) Li, Y.; Zhou, W.; Wang, H.; Xie, L.; Liang, Y.; Wei, F.; Idrobo, J.-C.; Pennycook, S. J.; Dai, H. *Nat. Nanotechnol.* **2012**, *7*, 394.
(12) Winther-Jensen, B.; Winther-Jensen, O.; Forsyth, M.; MacFarlane, D. R. *Science* **2008**, *321*, 671.
(13) Zheng, Y.; Jiao, Y.; Chen, J.; Liu, J.; Liang, J.; Du, A.; Zhang, W.; Zhu, Z.; Smith, S. C.; Jaroniec, M.; Lu, G. Q.; Qiao, S. Z. *J. Am. Chem. Soc.* **2011**, *133*, 20116.
(14) Yu, D.; Nagelli, E.; Du, F.; Dai, L. *J. Phys. Chem. Lett.* **2010**, *1*, 2165.
(15) Gong, K.; Du, F.; Xia, Z.; Durstock, M.; Dai, L. *Science* **2009**, *323*, 760.
(16) Tang, Y. F.; Allen, B. L.; Kauffman, D. R.; Star, A. *J. Am. Chem. Soc.* **2009**, *131*, 13200.
(17) Qu, L.; Liu, Y.; Baek, J.-B.; Dai, L. *ACS Nano* **2010**, *4*, 1321.
(18) Chen, S.; Bi, J. Y.; Zhao, Y.; Yang, L. J.; Zhang, C.; Ma, Y. W.; Wu, Q.; Wang, X. Z.; Hu, Z. *Adv. Mater.* **2012**, *24*, 5593.
(19) Yoo, E.; Nakamura, J.; Zhou, H. *Energy Environ. Sci.* **2012**, *5*, 6928.
(20) Yu, D.; Zhang, Q.; Dai, L. *J. Am. Chem. Soc.* **2010**, *132*, 15127.
(21) Yang, L.; Jiang, S.; Zhao, Y.; Zhu, L.; Chen, S.; Wang, X.; Wu, Q.; Ma, J.; Ma, Y.; Hu, Z. *Angew. Chem., Int. Ed.* **2011**, *50*, 7132.
(22) Wang, S.; Iyyamperumal, E.; Roy, A.; Xue, Y.; Yu, D.; Dai, L. *Angew. Chem., Int. Ed.* **2011**, *50*, 11756.
(23) Wang, S.; Zhang, L.; Xia, Z.; Roy, A.; Chang, D. W.; Baek, J.-B.; Dai, L. *Angew. Chem., Int. Ed.* **2012**, *51*, 4209.
(24) Grundmann, M. *The Physics of Semiconductors: An Introduction Including Nanophysics and Applications*; Springer-Verlag: Berlin, 2010; p 206.
(25) Kundu, S.; Xia, W.; Busser, W.; Becker, M.; Schmidt, D. A.; Havenith, M.; Muhler, M. *Phys. Chem. Chem. Phys.* **2010**, *12*, 4351.
(26) Vos, M.; Broek, A. D. European Patent EP 2199349A1, 2010.
(27) Jacobsohn, L. G.; Schulze, R. K.; Maia da Costa, M. E. H.; Nastasi, M. *Surf. Sci.* **2004**, *572*, 418.
(28) Ozaki, J.; Anahara, T.; Kimura, N.; Oya, A. *Carbon* **2006**, *44*, 3358.
(29) Chen, H.; Yang, Y.; Hu, Z.; Huo, K.; Ma, Y.; Chen, Y.; Wang, X.; Lu, Y. *J. Phys. Chem. B* **2006**, *110*, 16422.
(30) Ci, L.; Song, L.; Jin, C.; Jariwala, D.; Wu, D.; Li, Y.; Srivastava, A.; Wang, Z. F.; Storr, K.; Balicas, L.; Liu, F.; Ajayan, P. M. *Nat. Mater.* **2010**, *9*, 430.
(31) Berns, D. H.; Cappelli, M. A. *Appl. Phys. Lett.* **1996**, *68*, 2711.
(32) Polo, M. C.; Martínez, E.; Esteve, J.; Andújar, J. L. *Diam. Relat. Mater.* **1998**, *7*, 376.
(33) Yu, L.; Pan, X.; Cao, X.; Hu, P.; Bao, X. *J. Catal.* **2011**, *282*, 183.
(34) Carter, E. A. *Science* **2008**, *321*, 800.
(35) Frisch, M. J.; et al. *Gaussian 09*, Revision A.02; Gaussian, Inc.: Wallingford, CT, 2009.
(36) Glendening, E. D.; Landis, C. R.; Weinhold, F. *WIREs Comput. Mol. Sci.* **2012**, *2*, 1.
(37) Khalfoun, H.; Hermet, P.; Henrard, L.; Latil, S. *Phys. Rev. B* **2010**, *81*, 193411.